

DOI:10.4067/S0718-221X2021005XXXXXX

## A NEW METHOD FOR DETERMINING AIR PERMEABILITIES OF WOOD-BASED PANELS

**Takashi Tanaka**<sup>1,\*</sup>

<sup>1</sup>College of Agriculture, Academic Institute, Shizuoka University, Shizuoka, Japan

\*Corresponding author: [tanaka.takashi@shizuoka.ac.jp](mailto:tanaka.takashi@shizuoka.ac.jp)

**Received:** March 01, 2020

**Accepted:** September 07, 2020

**Posted online:** September 07, 2020

### ABSTRACT

In this study, a new apparatus for measuring the air permeability of wood-based panel specimens without using water displacement was developed with the aim of decreasing the influence of variation in atmospheric pressure on permeability measurement. Validation experiments were conducted using plywood, oriented strand board (OSB), particleboard, and medium-density fiberboard (MDF) panels and a control specimen sealed with an epoxy resin. The background (leakage) flow of the apparatus was evaluated based on the experimental results of the control specimen. A methodology for the determination of air permeability based on Darcy's law for gases and the evaluated background flow rate was proposed. The results of the current study were compared with those obtained in a previous study, indicating that the new method provides valid measurements for wood-based panels with high and low air permeability. No significant influence of variation in atmospheric pressure on the experimental results was observed, suggesting that the proposed method is suitable for a long-term continuous experiment for evaluating a specimen with extremely low permeability.

**Keywords:** MDF, OSB, particleboard, plywood, pressure measurement.

26

## INTRODUCTION

27 Several methods for measuring the air permeability of wood have been developed (Resch  
28 and Echlund 1964; Choong and Fogg 1968; Petty and Puritch 1970; Perré 1987; Siau  
29 1995; Perré 2007; Ai 2017). Using these methods and similar methods, the air  
30 permeability of various wood species in various directions has been determined (Resch  
31 and Echlund 1964, Choong and Fogg 1968, Comstock 1970, Perré 1987, Matsumura *et*  
32 *al.* 1994, Fujii *et al.* 1997, Lihra *et al.* 2000, Rayirath and avramidis 2008, Tanaka *et al.*  
33 2015, Poonia *et al.* 2016, Taghiyari and Avramidis 2019).

34

35 The Rising-Water Volume Displacement method, which has been introduced as a simple  
36 apparatus for student use by Siau (1995), is suitable for woods of high and low  
37 permeability. Because of its simplicity and versatility, the method is employed not only  
38 for wood but also for several wood-based panels (Tanaka 2014). During the experiments  
39 for woods of very low permeability using this method, however, a long-term experiment  
40 is necessary in order to decrease the difficulty in measuring a small increase in water level  
41 inside a transparent glass tube before and after water displacement. Here, according to  
42 the author's experience, variation in atmospheric pressure during the experiment is quite  
43 influential on the readings of the water level inside the glass tube.

44 In this study, a new apparatus without using water displacement for measuring air  
45 permeability was built from common lab instruments with the intention of decreasing the  
46 influence of variation in atmospheric pressure on permeability assessment. Validation  
47 experiments were conducted using several wood-based panels, and the methodology for  
48 the determination of air permeability based on the experimental data was proposed. The  
49 determined air permeability was compared with the results obtained in a previous study  
50 (Tanaka 2014) and the validity of the proposed method was verified. The influence of  
51 variation in atmospheric pressure on permeability assessment and suitability for a long-  
52 term continuous experiment for the evaluation of specimens with extremely low  
53 permeability was discussed.

## 54 MATERIALS AND METHODS

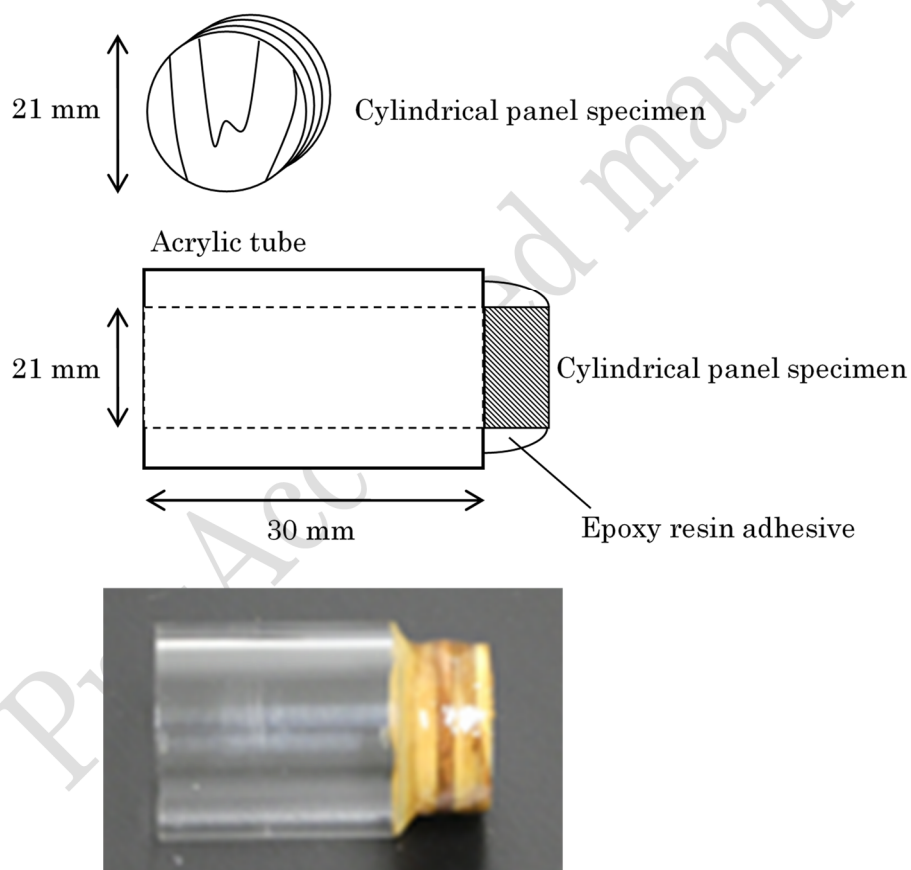
### 55 Sample preparation

56 Seven cylindrical wood-based panel specimens 21 mm in diameter (Table 1) were  
57 recalled from the previous experiment (Tanaka *et al.* 2014). All specimens were bonded  
58 with an acrylic tube 21 mm in diameter using an epoxy resin adhesive (Quick Set 30,  
59 Konishi Co. Ltd., Tokyo) (Figure 1) and had been stored in a climate room at 20 °C and  
60 65 % relative humidity. In the present study, an acrylic tube with a dead end with adhesive  
61 tape and epoxy resin was made as a control specimen (Figure 2).

62

**Table 1:** Testing panels.

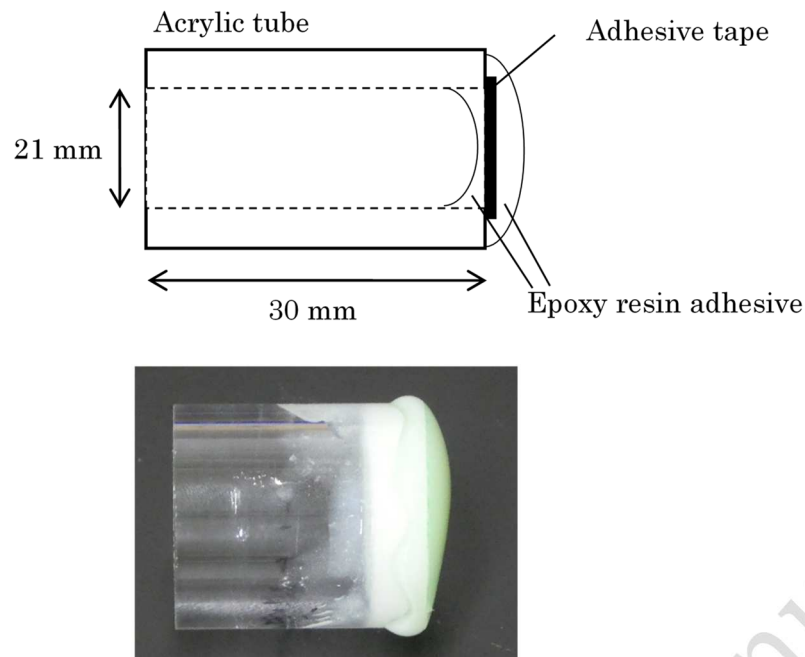
Panel Specimen	Thickness (mm)	Diameter (mm)	Ply	Air Permeability $k$ ( $10^{-12} \text{ m}^3/\text{m s Pa}$ ) (Tanaka 2014)
Plywood A ( <i>Cryptomeria japonica</i> )	11,68	21	5-ply	1,29
Plywood B ( <i>Larix kaempferi</i> )	12,69	21	5-ply	0,76
Plywood C ( <i>Larix gmelinii</i> )	12,35	21	5-ply	0,88
OSB U (made in EU)	9,6	21	-	67,9
OSB N (made in North America)	11,34	21	-	156
Particleboard	12,07	21	-	1780
MDF	12,08	21	-	23900



63

**Figure 1:** Schematic and photograph of the wood-based panel specimen.

64

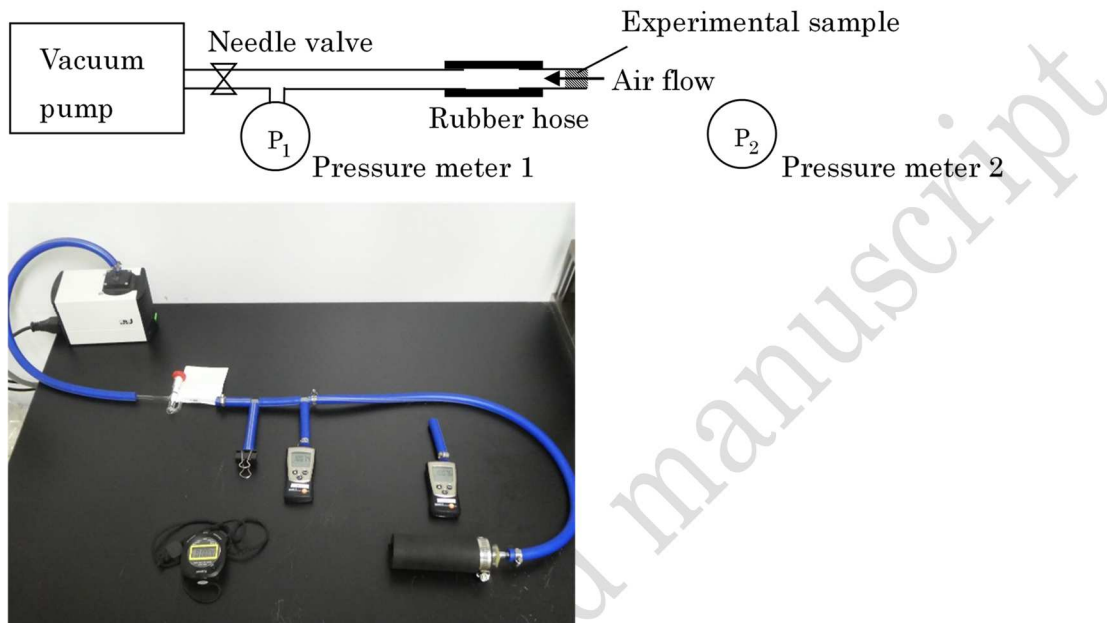


65  
66 **Figure 2:** Schematic and photograph of the control specimen.

67 **Experimental**

68 A new air permeability measurement system was built with two absolute pressure meters  
69 (Testo 511), a diaphragm vacuum pump (KNF Japan, N86KN.18), a needle valve, and  
70 rubber vacuum hoses of 6-mm and 25-mm internal diameter in a climate room at 20 °C  
71 and 65 % relative humidity (Figure 3). Each specimen was mounted to the end of the  
72 measurement system, and the vacuum pump was operated with the needle valve open.  
73 The valve was closed when the internal pressure of the system ( $p$ ) reached approximately  
74 700 hPa. The internal pressure ( $p$ ), atmospheric pressure ( $p_a$ ), and time ( $t$ ) were recorded  
75 every minute until  $t$  reached 15 min. The experiment for the control specimen was  
76 repeated 20 times over four days (Day 1–4): five runs on each day. The panel specimens

77 were tested on a day after two test runs using the control specimen. Here, the  $t-p$  curves  
78 of the MDF and particleboard cannot be recorded because of the excessive permeability  
79 to air.

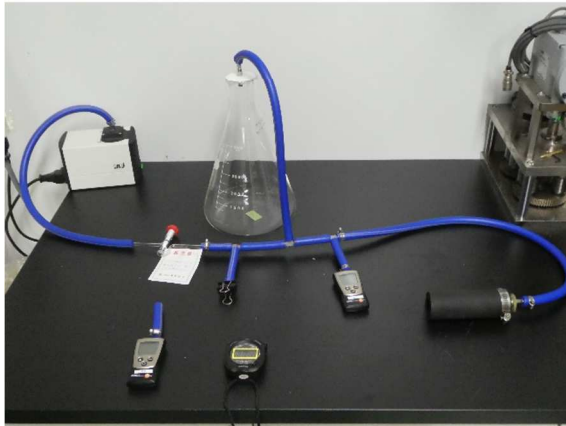
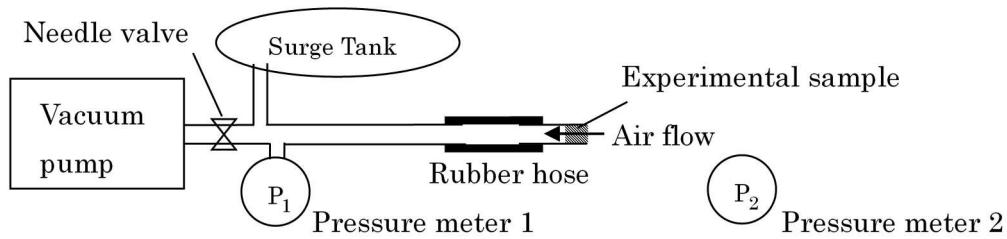


80 **Figure 3:** Schematic and photograph of the measurement system.

### 81 **Additional experiments with surge tank**

82 For the measurements of highly permeable panels (OSB, particleboard, and MDF), an  
83 additional surge tank (a conical flask with a capacity of 3000 mL) was installed between  
84 the needle valve and the internal pressure meter (Figure 4). All the panel specimens were  
85 tested on a day after two test runs using the control specimen.

86



87 **Figure 4:** Schematic and photograph of the measurement system with a surge tank.

88

### 89 **Long-term experiment of control specimen**

90 The control specimen was placed on the apparatus without the surge tank. The vacuum  
91 pump was operated with the needle valve open. The needle valve was closed when the  
92 internal pressure reached approximately 700 hPa. The internal and atmospheric pressures  
93 were recorded for 60 h.

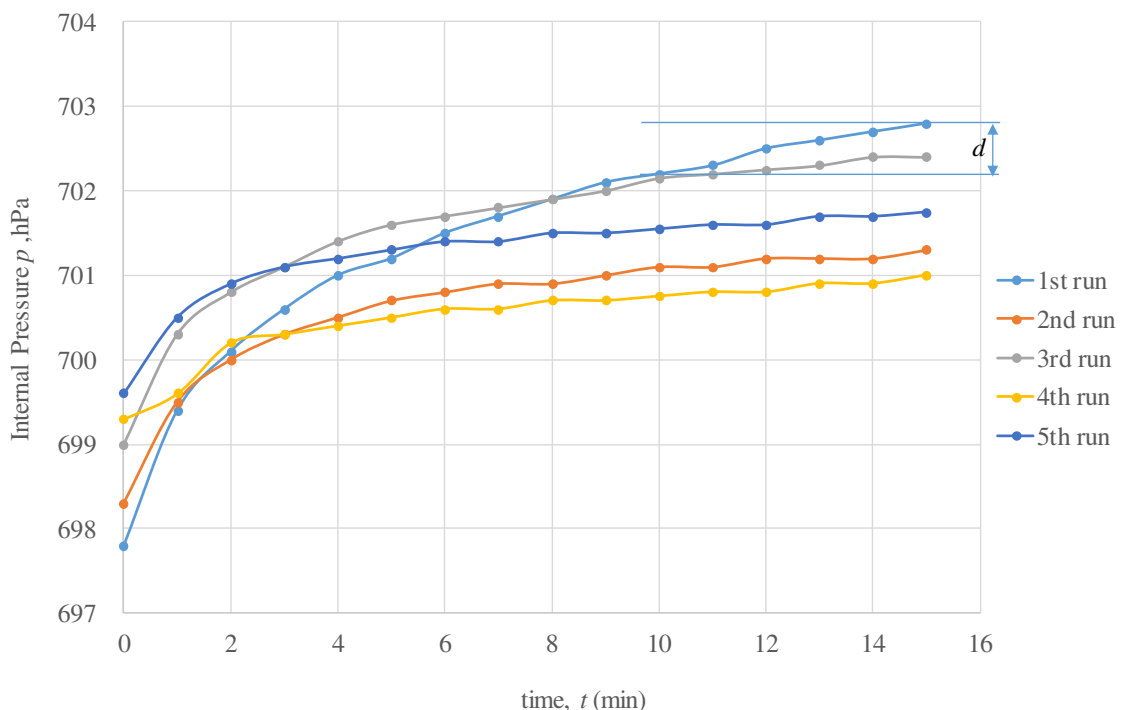
94

## **RESULTS AND DISCUSSION**

### 95 **Control specimen experiment results**

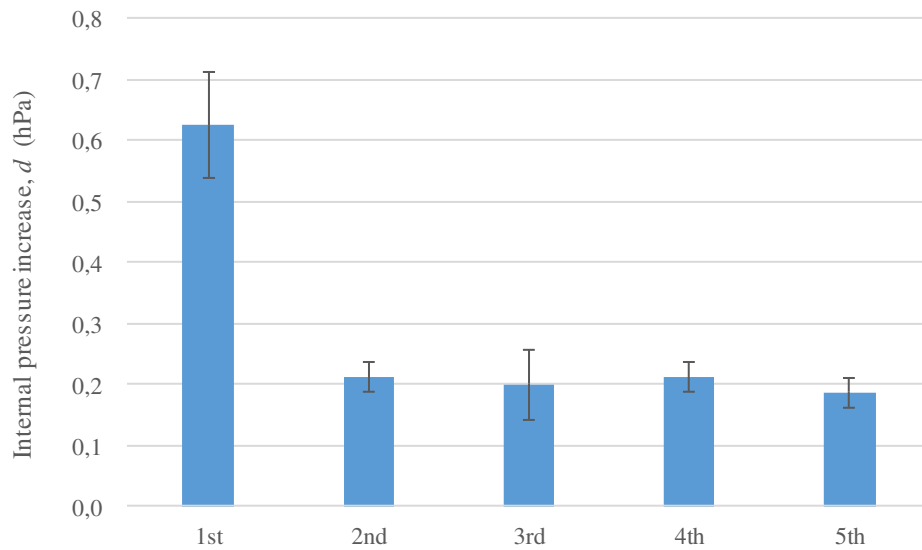
96 Figure 5 shows the relationship between the internal pressure of the experimental system

97 ( $p$ ) and time ( $t$ ) under the control specimen experiments on Day 1. The internal pressure  
98 of the system rapidly increased for the first few minutes of each run. Thereafter, the  
99 pressure increased, gradually decreased and became almost constant before  $t = 10$  min.  
100 Similar results were obtained on days 2–4. The results suggest that the pressure increase  
101 during the period from  $t = 10$  to  $t = 15$  ( $d$ ) provides an indication of the leakage flow into  
102 the experimental system. Furthermore, the pressure increase in the first run on any day  
103 was significantly larger than that in the 2nd-5th runs (Figure 6). Although the reason  
104 behind this phenomenon is unclear, the result of the first run on each day should be  
105 rejected as unsuitable for evaluation.



106  
107 **Figure 5:** Relationship between time ( $t$ ) and the internal pressure of the system ( $p$ ) in  
108 the control specimen experiment (Day 1).  
109





110 **Figure 6:** Influence of the repetition (1st–5th runs) of the control specimen experiment  
111 on the internal pressure increase from  $t = 10$  to  $t = 15$ .

112

### 113 **Evaluation of the leakage flow rate**

114 As mentioned above, the cause of the internal pressure increase of the experimental

115 system during the control specimen measurement is considered as the leakage flow into

116 the experimental system. Assuming that air is an ideal gas, the amount of air leaking into

117 the system during the period from  $t = 10$  to  $t = 15$  ( $n$ ) can be calculated using the following

118 equation:

$$119 \quad (100d)V_i = nRT \quad (1)$$

120 Solving for  $n$ ,

$$121 \quad n = \frac{(100d)V_i}{RT} \quad (2)$$

122 The leakage volume of air under atmospheric pressure  $V_{lk}$  is determined by the following

123 ideal gas equation:

$$124 \quad (100\bar{p}_a)V_{lk} = nRT \quad (3)$$

125 Substituting Equation (2) into Equation (3),

$$126 \quad V_{lk} = \frac{\frac{(100d)V_i}{RT} RT}{(100\bar{p}_a)} = \frac{dV_i}{\bar{p}_a} \quad (4)$$

127 The leakage flow rate  $Q_{lk}$  is obtained by dividing  $V_{lk}$  by the period of time:

$$128 \quad Q_{lk} = \frac{V_{lk}}{(60\Delta t)} = \frac{dV_i}{(60\Delta t)\bar{p}_a} \quad (5)$$

129 The leakage flow rate of each run was calculated using Equation (5). The average leakage  
130 flow rate from the 2nd to the 5th runs over the four-day experiments and the standard  
131 deviation was successfully obtained:

$$132 \quad \overline{Q_{lk}} = 0,000000000063 \quad (6)$$

$$133 \quad \sigma = 0,000000000011 \quad (7)$$

134

### 135 **Determination of air permeability of testing panels**

136 From Equations (4) and (5), the volume of air flow into the system  $V$  and the average  
137 flow rate  $Q$  are determined by the following equations:

$$138 \quad V = \frac{dV_i}{\bar{p}_a} \quad (8)$$

$$139 \quad Q = \frac{dV_i}{(60\Delta t)\bar{p}_a} \quad (9)$$

140

141 Figure 7 shows the relationship between the time and internal pressure of the system  
 142 during the panel specimen experiments. These increases in the internal pressure shown in  
 143 Figure 7 resulted from both the air flow through the panel specimen and from the leakage  
 144 of the system. Assuming the leakage flow rate is constant regardless of the specimen  
 145 material, the air flow rate through the panel during the period of time from  $t = 10$  to  $t =$   
 146  $15$  ( $Q_{\text{panel}}$ ) can be evaluated by subtracting the average leakage flow rate from the total  
 147 flow rate during the period of time from  $t = 10$  to  $t = 15$ :

$$148 \quad Q_{\text{panel}} = Q - \overline{Q}_{\text{lk}} \quad (10)$$

149 Air permeability can be calculated using Darcy's Law for gases (Siau 1995):

$$150 \quad k = \frac{Q_{\text{panel}} L (100 \overline{p}_a)}{A (100 \Delta p) \frac{(100 \overline{p}) + (100 \overline{p}_a)}{2}} \quad (11)$$

151 The pressure differential across panel  $\Delta p$  is calculated by subtracting  $\overline{p}$  from  $\overline{p}_a$ .

$$152 \quad \Delta p = \overline{p}_a - \overline{p} \quad (12)$$

153 Substituting Equations (10) and (12) into Equation (11), the following equation is  
 154 obtained:

$$155 \quad k = \frac{2L(Q - \overline{Q}_{\text{lk}}) \overline{p}_a}{A 100(\overline{p}_a - \overline{p})(\overline{p}_a + \overline{p})} \quad (13)$$

156 Here, the lower detection limit of  $Q_{\text{panel}}$  is chosen to be  $\overline{Q}_{\text{lk}} + 3\sigma$ . Thus, the air  
 157 permeability is determined using the following equations:

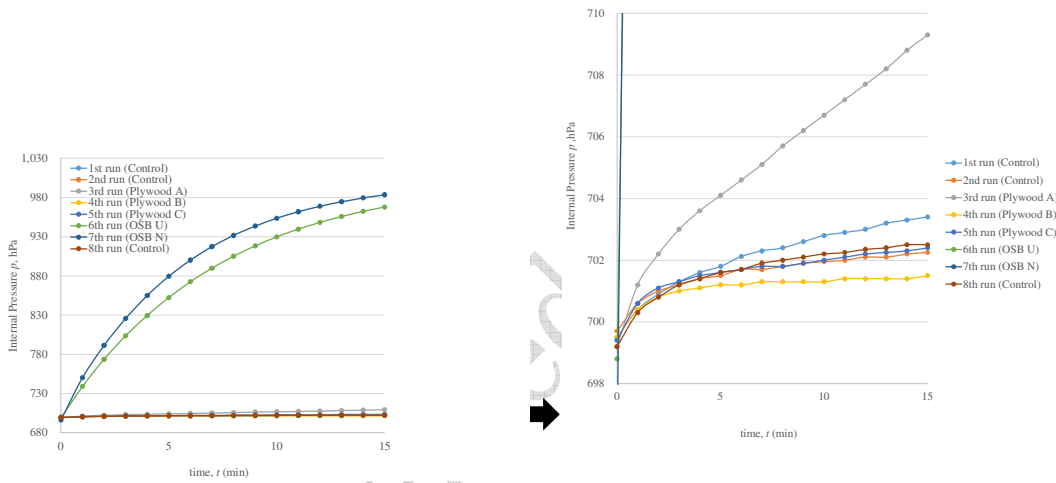
158 
$$k = \frac{2L(Q - \overline{Q}_{1k}) \overline{p}_a}{A 100(\overline{p}_a - \overline{p})(\overline{p}_a + \overline{p})} \quad (Q \geq 0,000000000096) \quad (14)$$

159 
$$k < \frac{2L(\overline{Q}_{1k} + 3\sigma) \overline{p}_a}{A 100(\overline{p}_a - \overline{p})(\overline{p}_a + \overline{p})} \quad (Q < 0,000000000096) \quad (15)$$

160 For the analysis of the well-permeable panels (OSB, particleboard, and MDF) using a  
 161 surge tank, the following equation is used:

162 
$$k = \frac{2LQ\overline{p}_a}{A 100(\overline{p}_a - \overline{p})(\overline{p}_a + \overline{p})} \quad (16)$$

163



164 **Figure 7:** Relationship between time and the internal pressure in the panel specimen  
 165 experiment.

166

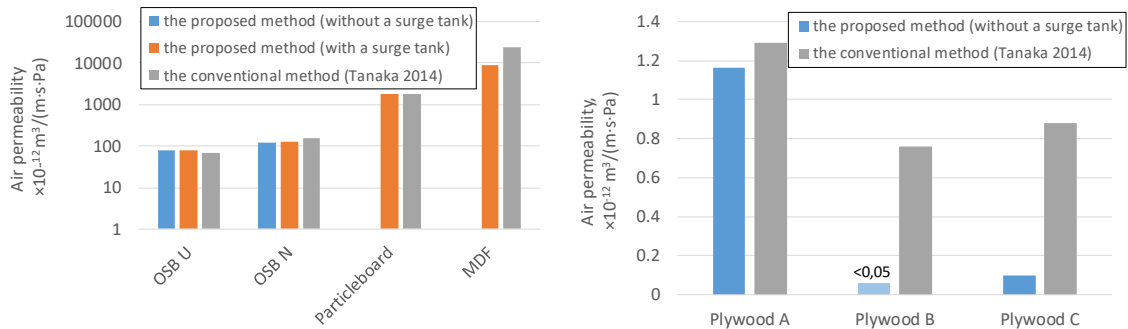
167 Figure 8a shows the air permeability of the panel specimens except for plywood,  
 168 indicating no significant difference between the results with and without a surge tank. The  
 169 use of a surge tank makes the proposed method suitable for a wood-based panel of higher  
 170 permeability. Moreover, there is no significant difference between the results determined  
 171 with the proposed method and the conventional method (Tanaka 2014). This indicates

172 that the method proposed in the present study can evaluate the air permeability of well  
173 permeable panels as accurate as the conventional method (Siau 1995).

174 Figure 8b shows the air permeability of the plywood panels. No significant difference  
175 was observed in Plywood A between the results determined in the present study and in  
176 the previous study (Tanaka 2014), whereas considerable differences were shown for  
177 Plywood B and Plywood C. In a previous study (Tanaka 2014), a 6-mm inner diameter  
178 measurement tube was used, and 10-minute multiple measurements of the control  
179 specimen were conducted to determine the background flow rate due to leakage. However,  
180 variation in atmospheric pressure during measurement influences the readings of change  
181 in water level. According to the Japan Meteorological Agency (2020), the average  
182 atmospheric pressure changes every 10 min in a city on a day was 0,13 hPa. Considering  
183 1 mmAq is equal to 0,1 hPa, atmospheric pressure variation during a 10-minute  
184 measurement in the previous study caused an average change of 1,3 mm in water level.  
185 This amount of change in water level is the equivalent of  $0,000000000061 \text{ m}^3/\text{s}$   
186 volumetric change ( $3 \times 3 \times 3,14 \times 1,3 \text{ mm}^3/600 \text{ s}$ ), which is much larger than the  $Q_{lk}$   
187 variation determined in the present study (Eq 7). This consideration leads us to conjecture  
188 that the method proposed in the present study is less affected by the atmospheric pressure  
189 variation and thus provides a more precise evaluation for wood-based panels with very

190 low permeability, such as plywood.

191



192

193 **Figure 8.** Air permeability of the testing panels. **a)** results of OSB, particleboard and MDF  
194 **b)** results of plywood.

195

### 196 **Robustness of the proposed method against variations in atmospheric pressure**

197 Figure 9a shows the changes in the internal pressure of the system and the atmospheric

198 pressure during the long-term experiment of the control sample. Figure 9b shows the

199 relationship between the atmospheric pressure change rate and the internal pressure

200 change rate. The coefficient of determination  $R^2$  was low, indicating that there is no

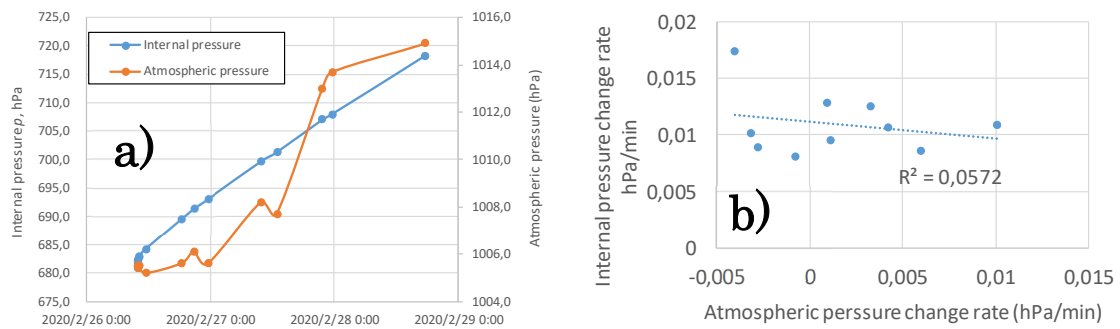
201 influence of variation in atmospheric pressure on the precision of the proposed method.

202 This robustness against atmospheric pressure change leads to precise measurement in a

203 long-term continuous experiment for the evaluation of specimens with extremely low

204 permeability.

205



206 **Figure 9.** Relationship between internal pressure and atmospheric pressure. **a)** changes  
207 in the internal and atmospheric pressures **b)** relationship between atmospheric pressure  
208 change rate and the internal pressure change rate.

209

210 Overall, the proposed method is more versatile in different wood-based panels than the  
211 conventional method (Siau 1995). It is probably applicable to solid wood and non-wood  
212 materials as well.

213

## CONCLUSIONS

214 In this study, a new method for determining the air permeability of wood-based panels  
215 without using water displacement was proposed. It is as valid as the conventional  
216 method for measuring air permeability in materials over a wide range of air permeability.

217 It also provides a rigorous measurement against variation in atmospheric pressure,  
218 suggesting that the proposed method is suitable for a long-term continuous experiment

219 for the evaluation of a specimen with even lower permeability.

220

221

222

## REFERENCES

223 **Ai, W., Duval, H., Pierre, F., Perré, P. 2017.** A novel device to measure gaseous  
224 permeability over a wide range of pressures: characterisation of slip flow for Norway  
225 spruce, European beech and wood-based materials. *Holzforschung* 71: 147-162.  
226 <https://doi.org/10.1515/hf-2015-0264>

227

228 **Comstock, G.L. 1970.** Directional permeability of softwoods. *Wood Fiber Sci* 1(4): 283–  
229 289. <https://www.fpl.fs.fed.us/documnts/pdf1970/comst70a.pdf>

230

231 **Choong, E.T.; Fogg, P.J. 1968.** Moisture movement in six wood species. *For Prod J*  
232 18(5): 66–70.

233

234 **Fujii, T.; Suzuki, Y.; Kuroda, N. 1997.** Bordered pit aspiration in the wood of  
235 *Cryptomeria japonica* in relation to air permeability. *IAWA J* 18(1): 69–76.  
236 <https://doi.org/10.1163/22941932-90001462>

237

238 **Japan Meteorological Agency. 2020.** Statistics in Shizuoka City on June 30th, 2020.  
239 [http://www.data.jma.go.jp/obd/stats/etrn/view/10min\\_s1.php?prec\\_no=50&block\\_no=4](http://www.data.jma.go.jp/obd/stats/etrn/view/10min_s1.php?prec_no=50&block_no=47656&year=2020&month=06&day=30&view=p1)  
240 [7656&year=2020&month=06&day=30&view=p1](http://www.data.jma.go.jp/obd/stats/etrn/view/10min_s1.php?prec_no=50&block_no=47656&year=2020&month=06&day=30&view=p1)

241

242 **Lihra, T.; Cloutier, A.; Zhang, S.Y. 2000.** Longitudinal and transverse permeability of  
243 balsam fir wet wood and normal heartwood. *Wood Fiber Sci* 32(2): 164–178.  
244 <https://wfs.swst.org/index.php/wfs/article/view/1581>

245

246 **Matsumura, J.; Tsutsumi, J.; Oda, K. 1994.** Relationships of bordered pit aspiration to  
247 longitudinal gas permeability in a given stem level: preliminary discussion on air-dried  
248 wood of *Cryptomeria japonica* and *Larix leptolepis* (in Japanese). *Bull Kyushu Univ For*  
249 71: 35–46. <https://doi.org/10.15017/10935>

250

251 **Perré, P. 1987.** Measurements of softwoods' permeability to air: importance upon the  
252 drying model. *Int Commun Heat Mass Transf* 14: 519–529. [https://doi.org/10.1016/0735-](https://doi.org/10.1016/0735-1933(87)90016-9)  
253 [1933\(87\)90016-9](https://doi.org/10.1016/0735-1933(87)90016-9)

254 **Perré, P. 2007.** Fluid migration in wood. In: Perré, P. (ed) *Fundamentals of wood drying*.  
255 A.R.BO.LOR., Nancy, France, pp. 125–156.

256



- 257 **Petty, J.A.; Puritch, G.S. 1970.** The effects of drying on the structure and permeability  
258 of the wood of *Abies grandis*. *Wood Sci Technol* 4: 140–154.  
259 <https://doi.org/10.1007/BF00365299>  
260
- 261 **Poonia, P.K.; Hom, S.K.; Sihag, K.; Tripathi, S. 2016.** Effect of microwave treatment  
262 on longitudinal air permeability and preservative uptake characteristics of chir pine wood.  
263 *Maderas-Cienc Tecnol* 18(1): 125–132. [http://dx.doi.org/10.4067/S0718-](http://dx.doi.org/10.4067/S0718-221X2016005000013)  
264 [221X2016005000013](http://dx.doi.org/10.4067/S0718-221X2016005000013)  
265
- 266 **Rayirath, P.; Avramidis, S. 2008.** Some aspects of western hemlock air permeability.  
267 *Maderas-Cienc Tecnol* 10(3): 185–193. [http://dx.doi.org/10.4067/S0718-](http://dx.doi.org/10.4067/S0718-221X2008000300002)  
268 [221X2008000300002](http://dx.doi.org/10.4067/S0718-221X2008000300002)  
269
- 270 **Resch, H.; Echlund, B.A. 1964.** Permeability of wood-exemplified by measurements on  
271 redwood. *For Prod J* 14(5): 199–206.  
272
- 273 **Siau, J.F. 1995.** Permeability. In *Wood: influence of moisture on physical properties*. Siau,  
274 J.F. (ed.). Virginia Polytechnic Institute and State University, Blacksburg NY, USA, pp.  
275 39–58.  
276
- 277 **Taghiyari, H.R.; Avramidis, S. 2019.** Specific gas permeability of normal and  
278 nanosilver-impregnated solid wood species as influenced by heat-treatment. *Maderas-*  
279 *Cienc Tecnol* 21(1): 89–96. <https://doi.org/10.4067/S0718-221X2019005000108>.  
280
- 281 **Tanaka, T. 2014.** Determination of the air permeabilities of wood-based panels in the  
282 through-thickness direction by using rising-water volume displacement method. (in  
283 Japanese) *Mokuzai Kogyo* 69(12): 589–593.  
284
- 285 **Tanaka, T.; Kawai, Y.; Sadanari, M.; Shida, S.; Tsuchimoto, T. 2015.** Air permeability  
286 of sugi (*Cryptomeria japonica*) wood in the three directions. *Maderas-Cienc Tecnol*  
287 17(1): 17–28. <http://dx.doi.org/10.4067/S0718-221X2015005000002>.  
288
- 289
- 290

291

## LIST OF SYMBOLS

- 292  $A$ : panel area ( $\text{m}^2$ )  
293  $d$ : the internal pressure increase during the period  $t = 10$  to  $t = 15$  (hPa)  
294  $k$ : air permeability ( $\text{m}^3/\text{m Pa s}$ )  
295  $L$ : thickness of panel (m)  
296  $n$ : the leakage amount of air during the period of time from  $t = 10$  to  $t = 15$  (mol)  
297  $p$ : internal pressure (hPa)  
298  $\bar{p}$ : average internal pressure during time  $t = 10$  to  $t = 15$  (hPa)  
299  $\Delta p$ : pressure differential across panel (hPa)  
300  $p_a$ : atmospheric pressure (hPa)  
301  $\bar{p}_a$ : average atmospheric pressure during time  $t = 10$  to  $t = 15$  (hPa)  
302  $Q$ : flow rate into the system under atmospheric pressure during the period  $t = 10$  to  $t = 15$   
303 ( $\text{m}^3/\text{s}$ )  
304  $\bar{Q}$ : Average leakage flow rate into the experimental system ( $\text{m}^3/\text{s}$ )  
305  $Q_{lk}$ : the leakage flow rate into the system during time  $t = 10$  to  $t = 15$  ( $\text{m}^3/\text{s}$ )  
306  $R$ : gas constant ( $\text{J}/\text{mol} \cdot \text{K}$ )  
307  $T$ : temperature (K)  
308  $t$ : time (min)  
309  $\Delta t$ : time from  $t = 10$  to  $t = 15$  (min)  
310  $V$ : the volume of air flow into the system under atmospheric pressure during the period  $t$   
311  $= 10$  to  $t = 15$  ( $\text{m}^3$ )  
312  $V_i$ : internal volume of the system ( $\text{m}^3$ )  
313  $V_{lk}$ : the leakage volume of air under atmospheric pressure during the period  $t = 10$  to  $t =$   
314  $15$  ( $\text{m}^3$ )  
315  $\sigma$ : standard deviation of the leakage flow rate ( $\text{m}^3/\text{s}$ )  
316